

## §8 Experiments with FRDC Source

### 8. 1 Introduction

The relation between the thermoelectric transfer difference and a FRDC-DC difference measurement has been discussed in the previous chapters §6 and §7. In this chapter, results of the experiment using the new FRDC source are reported. Results of the FRDC-DC difference measurements for different kinds of SJTCs and MJTCs are given in section 8.2, and the physical significance of the measured time-constant of the thermoelectric effect is discussed.

In the FRDC-DC difference measurements for the SJTCs and MJTCs, some types of TCs showed differences in the thermoelectric transfer difference between voltage and current mode as large as some parts in  $10^6$ . In order to investigate the origin of the discrepancy, the change of the thermoelectric transfer difference with the value of a resistor in series to the thermal converter has been measured. The results of the measurements and a possible explanation for the origin of the mode-dependence are described in section 8.3.

Since it is possible to evaluate thermoelectric transfer difference, the FRDC method may be used as an independent basis for ac-dc transfer standard. In this case, the evaluation of the uncertainty in the FRDC-DC difference measurement becomes important. The uncertainty has been estimated in detail for type-A and type-B components in section 8.4.

### 8. 2 Evaluation of thermoelectric effects

For the investigation of the origins of the thermoelectric transfer difference, the useful information obtained by the FRDC-DC difference measurement of the TCs are as follows;

- (a) Time constants of the thermoelectric effect which is estimated using the formula (6.15). From the thermoelectric time-constant, characteristic scale of thermoelectric effect is estimated using the formula (6.19) or (6.22).
- (b) Mode dependence of the thermoelectric effect. Different thermoelectric transfer difference may be observed for the voltage-mode and the current-mode measurement. For example, the EMF outside the heater does not affect the measurement in the current modes.
- (c) Input-level dependence of the thermoelectric effect. The ac-dc difference due to Thomson effect is proportional to the square of the input voltage/current level, as is shown in the equations (7.9). In the case of Peltier effect, the thermoelectric transfer difference is independent to the input level.

In this section, the results of the determination of ther-

moelectric transfer difference for SJTCs and MJTCs will be analyzed using the clues described above. In addition, an experimental evaluation of the reversal error in a SJTC is also described.

#### 8. 2. 1 Measurement system

A typical measurement system consists of a controller, a nano-voltmeter (Keithley 182), and a thermal converter to be evaluated. The schematic diagram and the photograph of the system are shown in **figure 8.1** and **8.2**, respectively. A lap-top PC is preferred as the controller, since the LCD display produces less noise than the CRTs, and it can be temporarily disconnected from the ac-power line to check the noise through the ac-power line.

The measurement procedure of a FRDC-DC difference measurement is basically the same as that for the ac-dc difference measurement except that the following two additional functions are required in the control program;

- (a) Adjustment of the 'dummy' resistor. This function is necessary in order to avoid overloading the source or dummy resistor. The program automatically sets the value of the dummy resistance to the same value as the input resistance of the TC/TVC to be measured with 100  $\Omega$  resolution.
- (b) Relative adjustment of the output level of the four sources ( $A\pm/B\pm$ ). The program automatically adjusts the relative output level with 10 ppm resolution.

A flow-chart of the automated measurement program is shown in **figure 8.3**. After the initialization, the program measures the normalized index "n" of the TC. The program also monitors the drift of the output EMF of the TC, and the index-measurements are repeated until the drift is stabilized within a specified value.

In the next stage, the program tries to adjust the four sources so that output EMF from the TC becomes equal for all the steady-state output mode. These adjustments are repeated until the output EMFs are adjusted within 20 ppm.

After completing the adjustment, the program goes to the main measurement sequence. The program uses the measurement sequence [ $*+/-/+*$ ], where the symbols represent;

- [ \* ] : Modified FRDC (A+/B-) : MDFR[1] mode
- [ + ] : Chopped dc (A+/B+) : CPDC[+] mode
- [ - ] : Chopped dc (A-/B-) : CPDC[-] mode
- [ / ] : Modified FRDC (A-/B+) : MDFR[2] mode

In each mode, the output EMF of the TC is measured by the Keithley 182 nano-voltmeter, and the data are averaged for specified number of reading. Then the FRDC-DC differ-

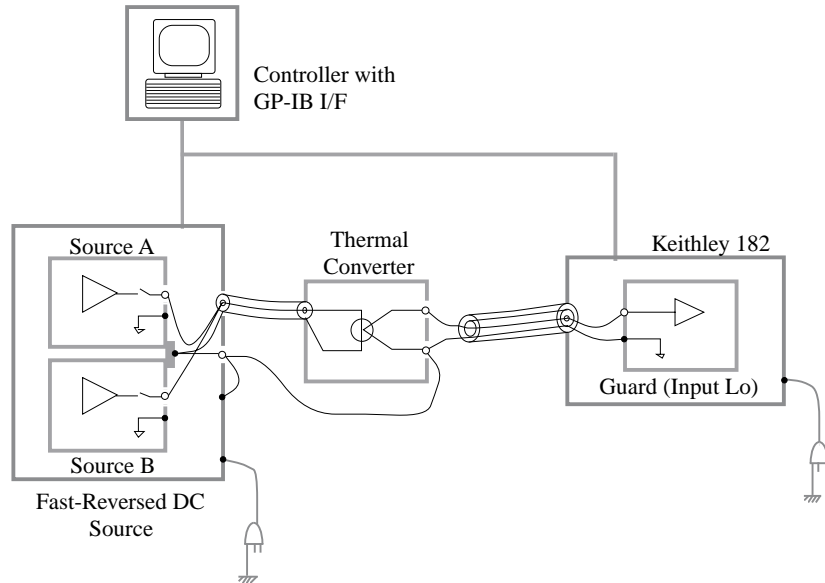


**Figure 8.1** The schematic diagram of the measurement system. The system consists of a controller, a nano-voltmeter (Keithley 182), and a thermal converter to be evaluated.



**Figure 8.2** Front view of the measurement system. A laptop PC is used as a system-controller.

ence is calculated using the formula (1.7) and (6.1) described in section 6.2.

### 8. 2. 2 Example of data for single-junction TCs

In the NML/CSIRO, single-junction TCs (SJTCs) have been used as a primary ac-dc transfer standard. A group of special TCs made with different design and materials have been developed at the NML. The TCs were extensively evaluated both experimentally and theoretically [10,11]. In order to evaluate the FRDC source using these special TCs, one of the production-model FRDC source was brought to the NML/CSIRO of Australia in 1995. Then the collaborative research has been performed for a period of two months.

In this section, typical results from the FRDC-DC difference measurement for the specially designed TCs will be presented. The measurement system consists of a FRDC source, EM null detector, Lindek potentiometer, and a Keithley 182 voltmeter for interfacing the null detector. The system was controlled by a PC-AT compatible with control software written in Pascal. The time-constants for joule heating were measured by changing the input level for 0.1 % and measuring the exponential response time. The thermoelectric

difference  $\delta_{TE}$  and the time-constant  $\tau_{TE}$  for the thermoelectric effect was determined by fitting the frequency dependence of the FRDC-DC difference using equation (6.15). The measurements were performed in a frequency range from 0.1 Hz to 1 kHz and at three different input-current levels.

#### (1) SJTC[#S6-8]

The SJTC [#S6-8] is made by Prosser Scientific Instrument. It has 55 ohm evanohm heater with epoxy bead. **Figure 8.4** shows the results from the FRDC-DC difference measurement for the TC. The TC has very small ac-dc difference of -0.2 ppm, and the dependence to the current level was within the detection sensitivity at 3 mA and 6 mA. The solid curve in the figure represents a theoretical curve fitting for 10 mA using equation (6.15). The time-constants for thermoelectric effect are measured to be 0.2 s, but it is not accurate due to very small value of thermoelectric transfer difference.

#### (2) SJTC[#S10-28]

The SJTC [#S10-28] is made by Best Products. It has 25 ohm evanohm heater with traditional 'flux' bead. The heater / heater-support junctions are also covered with pads made with flux. These pads are intended to reduce the effect from the Peltier heating at the heater / heater-support junctions, and are called "Peltier pads". **Figure 8.5** shows the results from the FRDC-DC difference measurement for the TC. It has the simple frequency dependence that can be fitted by single time-constant of 0.16 s. The FRDC-DC difference shows the simple quadratic current dependence; -1.6 ppm at 2.5 mA, -2.1 ppm at 5 mA and -2.9 ppm at 10 mA.

#### (3) SJTC[#S10-45]

The SJTC [#S10-45] is also from Best Products. It has the same design as the S10-28. The FRDC-DC

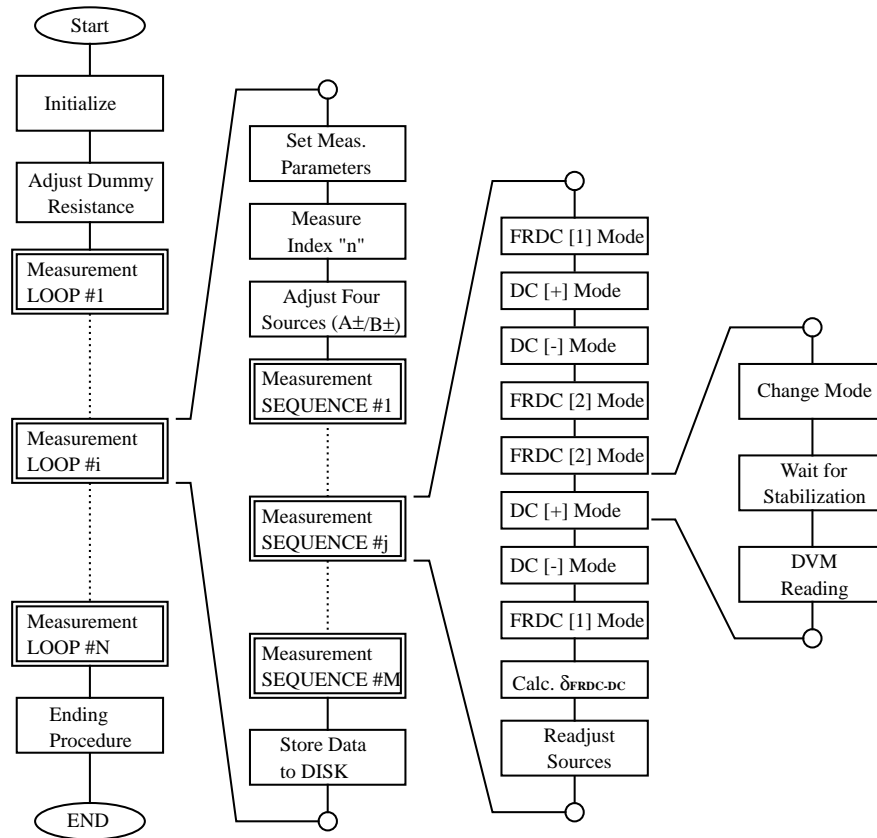


**Figure 8.3** Flow-chart of the automated measurement program. The measurement procedure of a FRDC-DC difference measurement is basically the same as that for the ac-dc difference measurement.

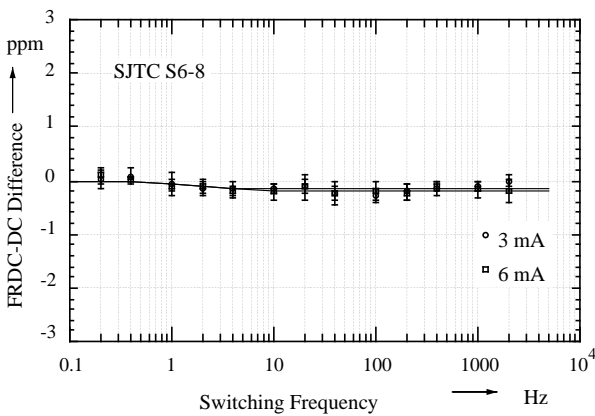


**Figure 8.4** Data from FRDC-DC difference measurement for a SJTC with epoxy bead (#S6-8 from Prosser Scientific Instrument). The solid curve in the figure is the curve-fitting to the theory.

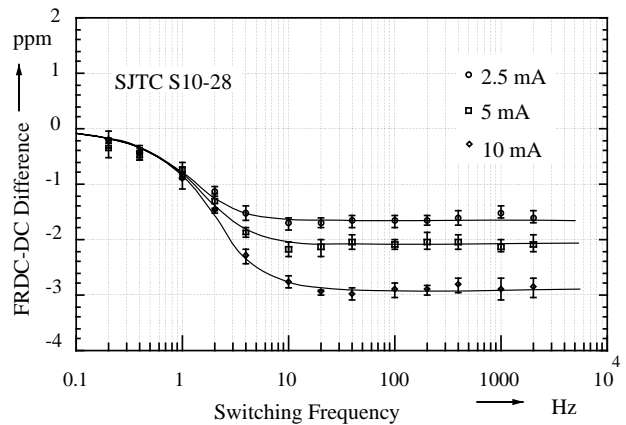


**Figure 8.5** Data from FRDC-DC difference measurement for a SJTC with ‘Peltier Pad’ at heater/support lead (#S10-28 from Best Products). The solid curve in the figure is the curve-fitting to the theory.

difference measurement for the TC is shown in **figure 8.6**. On contrary to the simple frequency dependence of #S10-28, #S10-45 does have the dual time-constant of 0.005 s and 0.25 s. This TC has noticeably small thermoelectric time constant of the order of milliseconds. Thermoelectric difference was measured to be -2.3 ppm at 5 mA and -2.6 ppm at 10 mA.

(4) SJTC[#S10-32]

The SJTC [#S10-32] is also from Best Products. It has similar design as the #S10-28 and #S10-45. It has 30 ohm evanohm heater with traditional ‘flux’ bead. It has ‘thermal guards’ near the end of the heater, so that the Peltier heat generated or absorbed at the heater / heater-support junctions should be conducted down to the base. The FRDC-DC difference measurement for the TC is shown in **figure 8.7**. In spite of this complex structure, it does have the simple

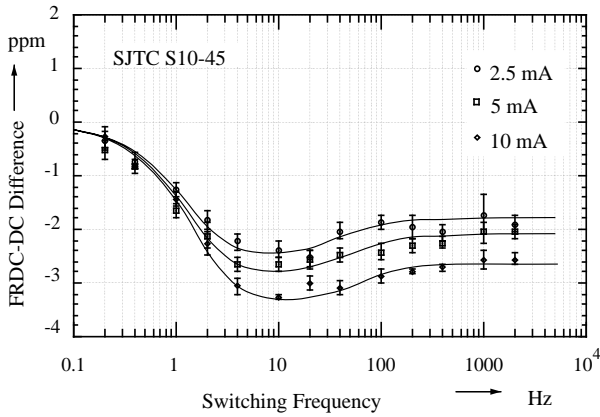


**Figure 8.6** Data from FRDC-DC difference measurement for a SJTC with the same construction as the S10-28 (#S10-45 from Best Products). The solid curve in the figure is the curve-fitting to the theory.

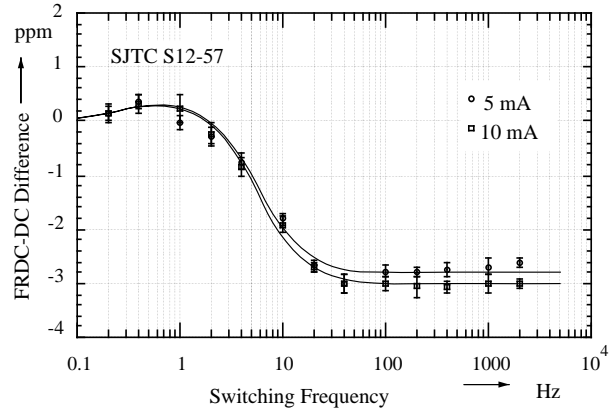


**Figure 8.8** Data from FRDC-DC difference measurement for a SJTC with ‘cold’ ceramic bead (#S12-57 from Vacuum Products). The solid curve in the figure is the curve-fitting

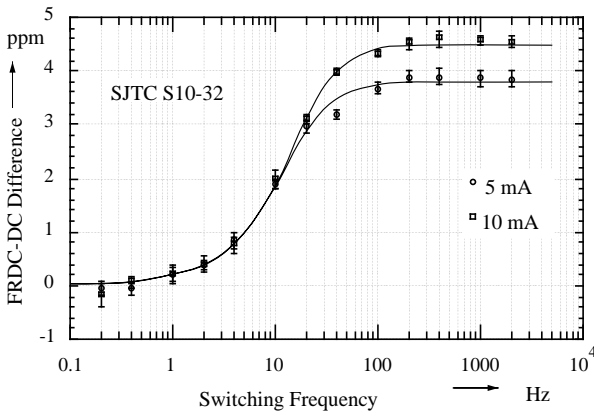


**Figure 8.7** Data from FRDC-DC difference measurement for a SJTC with ‘Thermal Guard’ at heater/support lead (#S10-32 from Best Products). The solid curve in the figure is the curve-fitting to the theory.

frequency dependence which can be fitted by single time-constant of 0.023 s. This TC shows positive thermoelectric transfer difference of +3.8 ppm at 5 mA and +4.6 at 10 mA.

(5) SJTC[#S12-57]

The SJTC [#S12-57] is from Vacuum Products. It has 25 ohm evanohm heater with ceramic bead. The ceramic bead is made with the ‘cold’ process in order to avoid local heating of the heater material by flaming, which may cause recrystallizing of the heater material and altering the Thomson constants. The TC has ‘thermal guards’ near the end of the heater as in the case of S10-32. The FRDC-DC difference measurement for the TC is shown in **figure 8.8**. Probably due to the complex structure, it has dual time-constant of 0.05 s and 0.9 s with different polarity. Thermal ac-dc difference was measured to be -2.7 ppm at 5 mA and -3.0 ppm at 10 mA.

One of the important result obtained from the five SJTCs is that there was a large dispersion in the thermoelectric time constant of SJTCs, as summarized in **table 8.1**. The TCs have similar dimensions and are made with similar design and materials. The time constants of joule heating were measured to be in the range  $1.2 \pm 0.5$  s. On the other hand, the thermoelectric time constants were distributed over two decades from 0.005 s to 2.2 s. The three TCs from the Best

**Table 8.1** Summary of results for measured Joule time constant and thermoelectric time constant of SJTCs. While the time constants of joule heating were measured to be in the range  $1.2 \pm 0.5$  s, the thermoelectric time constant spread over two decades from 0.005 s to 2.2 s.

	Thermoelectric Time Const.		Joule Time Const.		
	1st T.C.	( $\delta$ )	2nd T.C.	( $\delta$ )	
S6-8	0.2	-0.18			1.2
S10-28	0.16	-2.9			1.5
S10-45	0.25	-3.5	0.005	0.9	1.2
S10-32	0.023	4.6			1.7
S12-57	0.05	-3.7	0.9	0.7	0.7
	(s)	(ppm)	(s)	(ppm)	(s)

Product not only showed such dispersion in the thermoelectric time constant, but also different polarity in the thermoelectric transfer difference. These unexpected phenomena may be a clue for the investigation of the origin of the thermoelectric effects in the thermal converters.

### 8.2.3 Example of data for Multijunction TCs

The FRDC-DC differences of three types of MJTCs have been evaluated by using the FRDC source. The MJTCs are [#N136-1991] made by VNIIM, [PTB#249] and [PTB#73] made by PTB, and [GL#32472] made by Guildline Co. A small linear dependence on the switching frequency has been observed in the case of the MJTCs. As will be explained in the next section, the effects are probably due to the dielectric loss and/or absorption in the insulating material between the heater. Typical results from the MJTCs are as follows.

#### (1) MJTC[#N136-1991]

The MJTC[#N136-1991] is a 'T3m-6' type Multijunction TC, which is developed and manufactured at D.I. Mendeleyev Research Institute of Metrology (VNIIM), and is presently kept at NML/CSIRO. It has 100 ohm heater resistance and 10 mA nominal current. The time constant for the joule heating is measured to be 0.4 s. The FRDC-DC difference of the MJTC was measured with current-mode at the current level of 8 mA. The result is shown in **figure 8.9**. The measured data shows a linear frequency dependence, a typical characteristic for those MJTCs. The linear frequency dependence is also taken into account in the curve fitting of the data. The thermoelectric transfer difference is evaluated to be less than 0.1 ppm.

#### (2) MJTC[PTB#249]

The MJTC[PTB#249] is a Multijunction TC developed at PTB and presently maintained at NML/CSIRO. It has 198 ohm heater resistance and 3V nominal input voltage. The time constant for the joule heating is measured to be 1.5 s. The FRDC-DC difference of the MJTC was measured

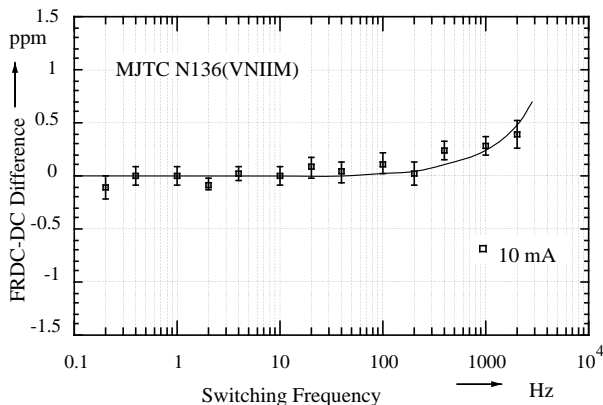


**Figure 8.9** Data from FRDC-DC difference measurement for a MJTC from VNIIM (#N136-1991 / Model-T3m-6 maintained at CSIRO/NML). The solid curve in the figure shows the linear-curve-fitting of the data.

with current-mode at the current level of 10 mA. The result is shown in **figure 8.10**. The linear frequency dependence is observed as in the case of #N136-1991. The thermoelectric transfer difference is evaluated to be less than 0.1 ppm.

#### (3) MJTC[PTB#73]

The MJTC[PTB#73] is a Multijunction TC developed at PTB and presently maintained at ETL. It has the same design as the [PTB#249]. The MJTC was measured at both voltage-mode (3 V/15 mA, 2 V/10 mA) and current-mode (10 mA). **Figure 8.11** shows the results from the FRDC-DC difference measurement for the MJTC. The linear frequency dependences are observed for both current-mode and voltage-mode. The thermoelectric transfer difference is evaluated to be less than 0.1 ppm for both of the modes.

#### (4) MJTC[GL#32472]

The MJTC[GL#32472] is a commercially available Multijunction TC from Guildline. As discussed in section 4.5.2, the MJTC has been estimated to have mode dependence of 2 ppm. The MJTC was measured at both voltage-mode (5 V) and current-mode (10 mA). **Figure 8.12** shows

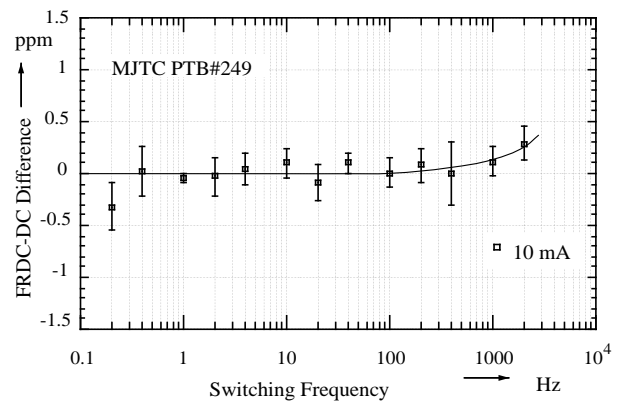


**Figure 8.10** Data from FRDC-DC difference measurement for a MJTC from PTB (PTB#249 maintained at CSIRO/NML). The solid curve in the figure shows the linear-curve-fitting of the data.

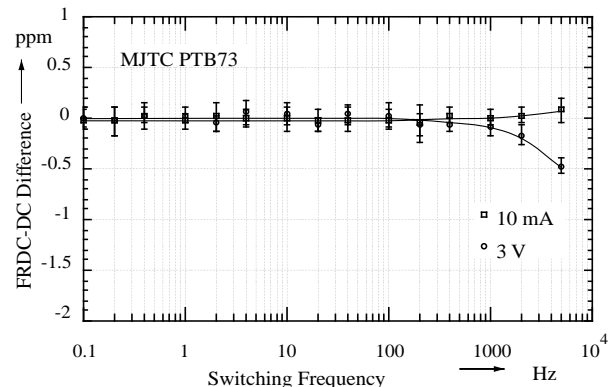


**Figure 8.11** Data from FRDC-DC difference measurement for a MJTC from PTB (PTB#73 maintained at ETL). The solid curve in the figure shows the linear-curve-fitting of the data.

the results from the FRDC-DC difference measurement for the TC. The thermoelectric transfer difference is evaluated to be less than 0.1 ppm for the current modes, and 2.0 ppm for the voltage mode. This result suggests the existence of thermal EMF voltage along the input circuit, probably outside the heater.

All the measurements for the MJTCs from PTB yielded results of FRDC-DC difference smaller than 0.1 ppm, as expected. On the other hand, some of the SJTCs measured at CSIRO showed differences of about 2 ppm between the theory and the measurement. These results imply that the discrepancy between the standard based on SJTC and the standard based on MJTC may be due to incompleteness of the theory. From the fact that some of the TCs showed the time constant of thermoelectric effect much smaller than the joule time constant, it is likely that the influence of local effect, which was not taken into account in the theory, contributed the non-negligible thermoelectric transfer difference.

On the other hand, while the thermoelectric transfer difference of SJTC(#S6-8) from Prosser Sci. Instrum. was measured to be -0.2 ppm, in close agreement with the estimated value, the MJTC(GL#32472) from Guildline showed thermoelectric transfer difference of -2 ppm in the voltage mode. Hence all the MJTCs are not necessarily superior to SJTC.

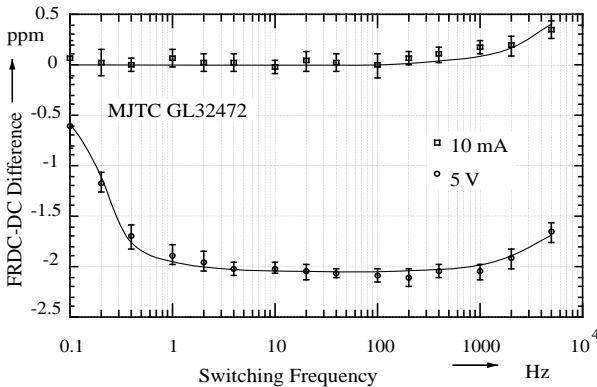


**Figure 8.12** Data from FRDC-DC difference measurement for a MJTC from Guildline (GL#32472 maintained at JEMIC). Difference of 2 ppm between voltage mode and current mode is observed. The solid curve in the figure is the fitting to the theory taking the linear dependence into account.

## 8. 2. 4 Reversal error measurement

The thermal converters produce different output EMF for positive and negative polarity of the input current due to the first-order thermoelectric effect. The difference in the output EMF for both polarities are called as ‘reversal error’ and are defined as;

$$\frac{\Delta I}{I} \equiv \frac{E(I_+) - E(I_-)}{nE_0} \quad (8.1)$$

In the ac-dc transfer difference and the FRDC-DC difference, the first-order effects are compensated by taking the mean of the output EMF for positive and negative polarity of the current, as described in section 6.2.1. Nevertheless, since the first-order effect is the origin of the second-order effect, it would be interesting to measure how the reversal error varies with the reversing frequency.

In this sub-section, an experimental-setup for measuring the frequency characteristic of the reversal error is described. The circuit diagram of measurement system is shown in **figure 8.13**. The FRDC source is set to the FRDC (A+/B-) mode. The difference in the output EMF for both polarities is obtained by the synchronous switching of the analog switch (AD7510). The reversal error is calculated by the following equation;

$$\begin{aligned} \frac{\Delta I}{I} &\equiv \frac{E(A+) - E(B-)}{nE_0} \\ &= \frac{\Delta E(A+) - \Delta E(B-)}{nE_0} \end{aligned} \quad (8.2)$$

We measure the compensated EMF ( $\Delta E$ ) so as to suppress the big voltage swing at the input of the low-pass filter.

The measurement was performed on a TC of old ETL-design (SN105921), which has a large thermoelectric transfer difference of -4 ppm. The result of the measurement is shown in **figure 8.14**. The measured value has unknown offset due to mismatching the output from the sources A+/B- and the uncompensated offset of the operational amplifiers. Below 0.5 Hz, a large effect from the thermal ripple is dominant due to unmatched output level between A+ and B-. Above 200 Hz, we get a deviation probably due to the effect from the analog switch or the reduced gain of the operational amplifiers. Assuming that the data between 0.5 Hz and 200 Hz reflects the thermoelectric effects, we obtain two time

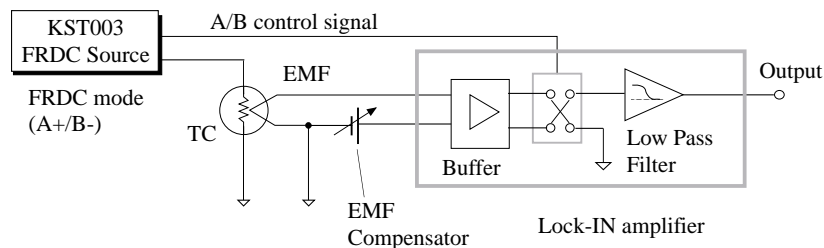


**Figure 8.13** An experimental-setup for measuring the frequency characteristic of the reversal error. Setting the FRDC source to the FRDC (A+/B-) mode, the reversal error is measured by the synchronous switching of the analog switches.

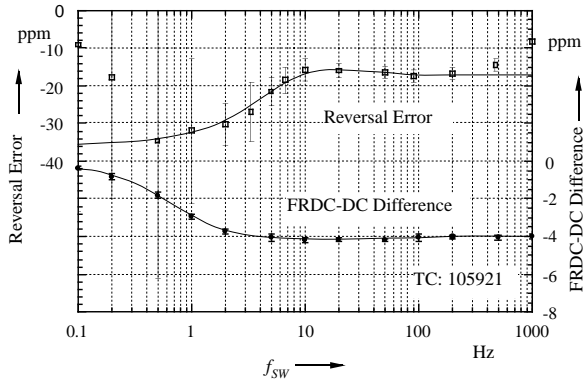


**Figure 8.14** The result of the reversal-error measurement. The measured value has unknown offset due to mismatching of the output from the sources A+ and B-. The time constant for the first-order thermoelectric effect is evaluated to be 0.068 s (25.6 ppm) and 0.016 s (-7.1 ppm), assuming that the data between 0.5 Hz and 200 Hz reflects the thermoelectric effects.

constants, (0.068 s, 25.6 ppm) and (0.016 s, -7.1 ppm) for the first-order thermoelectric effect.

On the other hand, different time constants, (0.44 s, -4.16 ppm) and (0.0024 s, 0.16 ppm) were obtained from the FRDC-DC difference measurement. The difference in the major time-constants for the first-order and the second-order effect may be explained by the simulation described in section 7.4.5. In the simulation, the thermoelectric effect due to local Peltier effect was evaluated. As was shown in the figure 7.13, the local Peltier effect could produce large first-order temperature variation of the order of a few hundred ppm near the vicinity of the bead. However, the second-order effect due to the local effect is largely compensated and reduced to be of the order of 0.1 ppm. Thus, the time constant of the first-order effect and the second-order effect may reflect different phenomena in the thermal converter.

### 8.3 Mode-dependence measurement

In the section 8.2, we have evaluated the thermoelectric effect of different types of TCs, including the SJTCs and multijunction thermal converters (MJTCs). The results obtained by the FRDC measurement were generally in good agreement with conventional ac-dc transfer standards based on theoretical evaluations of the thermoelectric transfer difference. However, in the measurements of some types of MJTCs, a discrepancy as large as some parts in  $10^6$  was observed in the thermoelectric transfer differences, depending on whether the measurements were performed in the voltage mode or in the current mode (“mode-dependence” of the thermoelectric transfer difference). The mode-dependence may be explained by thermoelectric voltages in the input circuit due to the Seebeck effect in the case of SJTC elements[3,4]. However, the mode-dependence was much larger than we anticipated for MJTCs. In most of the ac-dc transfer difference measurements, the TCs are used in combination

with range-resistors. In these cases, the measurement conditions are neither pure voltage mode nor pure current mode. The effect of the mode-dependence may become significant in the voltage step-up procedure, where TCs are combined with range-resistors of different values, and the accumulation of systematic errors may be possible in the step-up procedure.

In this section, we describe the result of FRDC-DC difference measurements on a SJTC and two MJTCs. The measurement was performed on different configurations of range resistor/ TC combinations, changing the value of the range resistor from zero (TC only) to infinity (current mode). The results were compared with a theoretical evaluation based on an assumption that the Seebeck effect is the main source of the voltage transfer difference.

#### 8.3.1 Mode-dependent FRDC-DC difference

The mode-dependencies of the thermoelectric transfer difference were investigated extensively for an SJTC and two MJTCs. The FRDC-DC difference measurement was performed both in the voltage and current mode, changing the reversing frequency from 0.05 Hz to 5 kHz. The results of the FRDC-DC difference measurement are shown in **figure 8.15**.

Figure 8.15 (a) shows the result for an SJTC (SN#TCJ94014C) used for the main working standard of JEMIC. The SJTC consists of four units of 10 mA, 25  $\Omega$  type-SS283 SJTC elements from Best-Technology Co. The thermoelectric transfer differences of the SJTC are measured to be  $-0.3 \times 10^{-6}$  in current mode and  $-2.4 \times 10^{-6}$  in voltage mode. This SJTC has two time-constants (2.5 s, 0.14 s) as shown by the fitted curve. Figure 8.15(b) represents the results for an MJTC (SN#32465) with 460  $\Omega$  input resistance, Guildline Instruments Type-7000. The thermoelectric transfer differences are measured to be  $< 10^{-7}$  in the current mode and  $-2.2 \times 10^{-6}$  in the voltage mode. Figure 8.15(c) represents the results for a type ‘T3m-6’ MJTC (SN#477) developed at the VNIIM. The thermoelectric transfer differences are measured to be  $< 10^{-7}$  in the current mode and  $-0.7 \times 10^{-6}$  in the voltage mode.

#### 8.3.2 Thermal EMF due to Seebeck effect

When the dc current  $I$  passes through the heater/heater support junctions of an SJTC, Peltier heating and cooling takes place at the junctions, as illustrated in **figure 8.16**. This effect results in a difference in temperature  $\Delta T$  between the two junctions, which can be calculated as

$$\Delta T = \frac{2\pi_{12}}{K_1 + 2K_h} \cdot I, \quad (8.3)$$

where

- $\pi_{12}$  relative Peltier coefficient between the support lead 1 and the heater 2,
- $K_1$  thermal conductance of the support lead from the heater end to the cold junction region,
- $K_h$  thermal conductance of the heater,

$I$  dc current applied to the thermal converter.

The temperature difference  $\Delta T$  generates the thermoelectric voltage  $\varepsilon_{12}$  due to the Seebeck effect [10,11]. The thermoelectric voltage  $\varepsilon_{12}$  between the input leads of the SJTC may be expressed approximately as

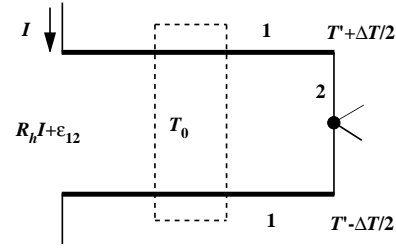


**Figure 8.16** Model for an SJTC with heater '2' and support leads '1'. The temperature difference  $\Delta T$  is produced by Peltier effect across the heater, which generates a thermoelectric voltage  $\varepsilon_{12}$  due to the Seebeck effect.

$$\varepsilon_{12} = S_c \cdot \Delta T = \frac{2S_c \pi_{12}}{K_1 + 2K_h} \cdot I. \quad (8.4)$$

Here  $S_c$  represents the Seebeck or thermoelectric coefficient of the heater/heater-support junctions. Since the thermoelectric voltage  $\varepsilon_{12}$  is proportional to current  $I$  and changes its polarity with current direction, we can define an effective resistance as  $\Delta R_{eff} \equiv \varepsilon_{12}/I$ . The contribution of the thermoelectric voltage to the ac-dc transfer difference  $\delta_{EMF}$  depends on the total voltage drop across the range resistor/ SJTC combination

$$\delta_{EMF} = \frac{-\varepsilon_{12}}{(R_h + R_r)I} = \frac{-\Delta R_{eff}}{(R_h + R_r)}$$

where

$$\Delta R_{eff} = \frac{2S_c \pi_{12}}{K_1 + 2K_h}. \quad (8.5)$$

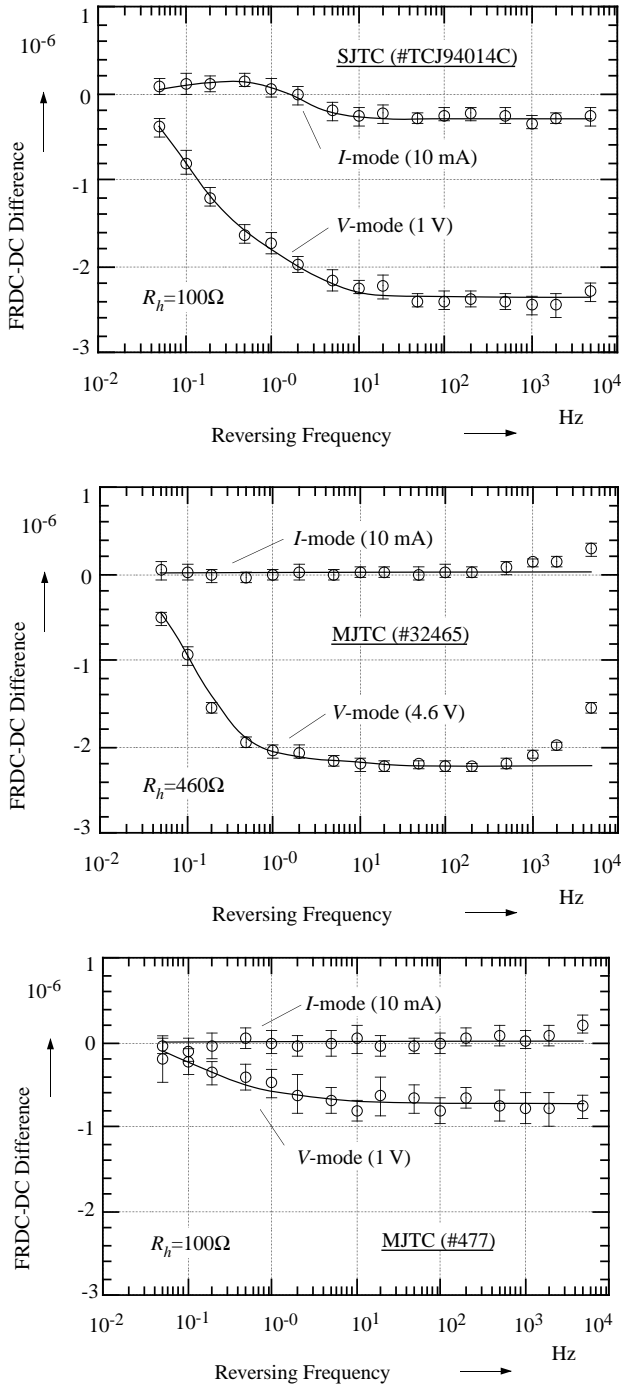
The resistance  $R_h$  and  $R_r$  represent the heater and the range resistor, respectively. The thermoelectric transfer difference  $\delta_{EMF}$  due to the Seebeck effect is expected to decrease with the total resistance  $R_h + R_r$ , and to be independent of the current.

In the case of a typical SJTC element, the thermal conductance  $K_1$  and the Seebeck coefficient are of the order of 0.3 mW/K and  $(5 \pm 6) \mu\text{V/K}$  respectively [10]. The thermal conductance of the heater  $K_h$  is assumed to be small compared with that of the support lead  $K_1$ . The effective resistance  $\Delta R_{eff}$  is estimated to be  $\leq 300 \mu\Omega$ , resulting in a thermoelectric transfer difference of a few parts in  $10^6$  in voltage mode.

### 8.3.3 Experimental results and discussion

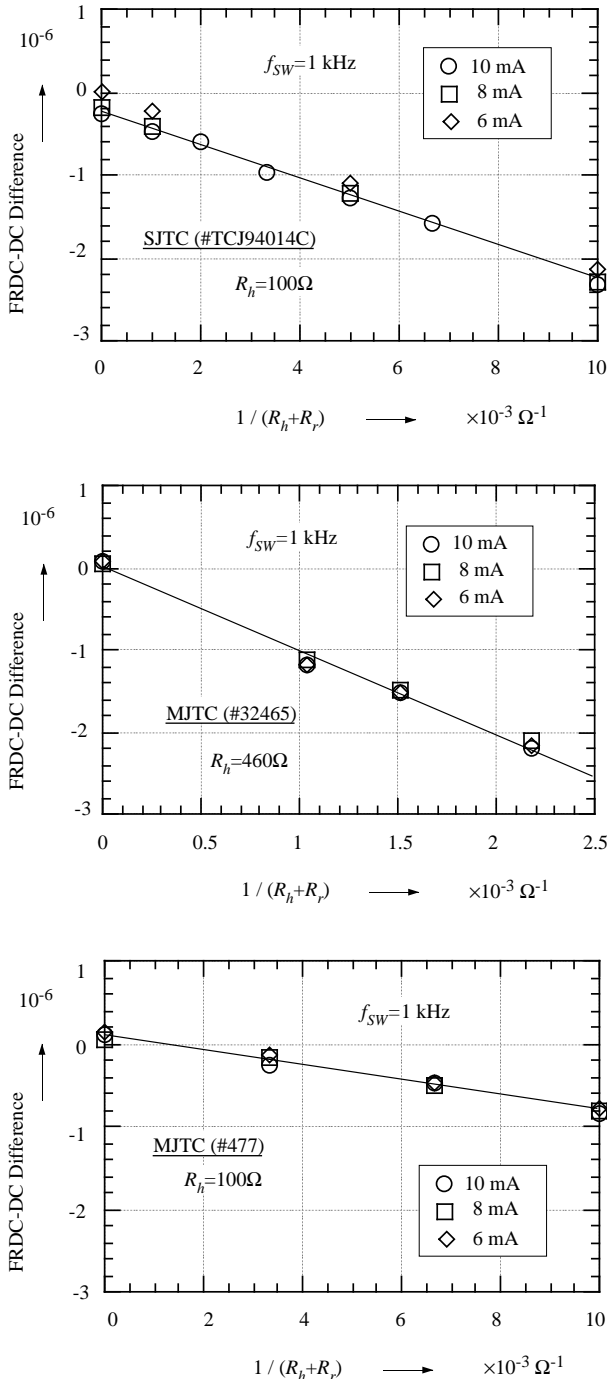
To test the adequacy of the mathematical model described above, the dependence of FRDC-DC voltage transfer differences  $\delta_{FRDC-DC}$  on the value of range resistors  $R_r$  was measured for the three TCs described in the previous section. The results are shown in **figure 8.17**. The horizontal axis represents the inverse of the total resistance [ $1/(R_h + R_r)$ ] in  $\Omega^{-1}$ .

Figure 8.17(a) shows the result of the FRDC-DC difference measurement for the SJTC(SN#TCJ94014C). The total resistance  $R_h + R_r$  was varied from 100  $\Omega$  to 1000  $\Omega$ . The data on the y-axis represent the data for current-mode



**Figure 8.15** Frequency characteristic of the FRDC-DC difference of thermal converters at voltage and current mode. (a) Result for an SJTC [SN#TCJ94014C] with four type-SS283 elements from Best Technology. (b) Result for an MJTC [SN#32465] from Guildline. (c) Result for a MJTC [SN#477] from VNIIM. The bars represent type-A uncertainties ( $3\sigma$ ) of the measurement.

measurements. Figure 8.17 (b) shows measurements for the MJTC (SN#32465) from Guildline. The total resistance  $R_h+R_r$  was varied from 460  $\Omega$  to 960  $\Omega$ . Figure 8.17 (c) shows measurements for the type ‘T3m-6’ MJTC (SN#477) from VNIIM. The total resistance  $R_h+R_r$  was varied from 100  $\Omega$  to 300  $\Omega$ .



**Figure 8.17** Variation of the FRDC-DC voltage transfer difference versus resistance of the range resistor/TC combination measured at different current levels (a) Result for a SJTC [SN#TCJ94014C] with four type-SS283 elements from Best Technology. (b) Result for an MJTC [SN#32465] from Guildline. (c) Result for an MJTC [SN#477] from VNIIM. The x-axis represents the inverse of the total resistance in  $\Omega^{-1}$ .

For all three TCs measured, the FRDC-DC voltage transfer differences showed linear dependence on the inverse of the total resistance [ $1/(R_h+R_r)$ ], as expected from (8.5). The FRDC-DC transfer difference was measured at current levels of 100 %, 80 %, and 60 % of the rated currents. In the case of SJTC (SN#TCJ94014C), a small current-level dependence of a few parts in  $10^6$  is observed. However, the dependence of the thermoelectric transfer difference on the total resistance was not affected by changing the current level, which is also in agreement with (8.5). These experimental results supports the assumption that the ac-dc voltage transfer difference originates from thermoelectric voltage due to the Seebeck effect.

## 8.4 Measurement uncertainties

Since the FRDC method may serve as an independent basis for ac-dc transfer standard, the evaluation of the uncertainty in the FRDC-DC difference measurement becomes important. In this section, the uncertainty will be estimated in detail for the measurement with the production model (KST003) FRDC source.

The sources of uncertainty for category-A evaluation consist of the following three parts;

- Instability of the rms output of the FRDC source.
- Fluctuation of the output EMF of the TC to be measured.
- The resolution of the detector.

Since the uncertainty for type-A evaluation depends on each measurement condition, the uncertainty has to be evaluated for each measurement using the standard deviation of the data.

The sources of uncertainty for category-B evaluation are as follows:

- Effect of imperfect switching.
- Memory-effect of analog switches.
- Mismatching dummy-load resistance.
- Interference between the two sources.
- Dielectric loss/absorption in the TC-input circuit.
- Effect of off-time.
- Finite output resistance of the source.
- Mismatching of rms power.
- Effect of higher frequency components.

The effect of slew rate and transients at the time of switching have been the major source of uncertainties in the case of original FRDC waveform. In the case of modified waveform, these effects are automatically compensated between the MDR and CPDC modes, as was discussed in section 4.2.3.

### 8.4.1 Type-A uncertainties

- Instability of FRDC output

Since the change in the output of the FRDC source causes the instability in the EMF output of the TCs, it may become a major source of type-A uncertainty. Instability of the new FRDC source is measured to be about 0.5 ppm (rms), as was

shown in the figure 5.9. In the measurement of FRDC-DC difference, the output is usually integrated for more than 60 seconds. Since the short-term fluctuation within this integration period averages out, contribution of the instability to the measured standard deviation is expected to reduce of the order of 0.1 ppm. In addition, the effect of linear drift in the output is also compensated by the standard measurement sequence [MDFR(1), CPDC(+), CPDC(-), MDFR(2)].

(2) Fluctuation of TC output

In the case of SJTCs, the temperature coefficients of the output EMFs are of the order of 100 ppm/K, which is much larger than that of the FRDC-source output. Though the linear component of the drift is compensated by the standard measurement sequence, the second-order component can still cause an error of more than 1 ppm. Hence the thermal guarding of the TC against the change of the ambient temperature is critically important for a precision measurement.

In addition to the effect of temperature variation, a fluctuation is contributed from the Johnson noise of the thermocouple of TC. If we use a standard-pattern SJTC, which has 10 Ω EMF output impedance, the Johnson noise of the thermocouple  $e_n$  is estimated as,

$$e_n(\text{rms}) \cong \sqrt{4 \times 1.38 \times 10^{-23} (J/K) \times 400(K) \times 10(\Omega)}$$

$$\cong 0.5 \text{ nV} / \sqrt{\text{Hz}}$$

In this case, the thermal noise from the TC is as small as 0.04 ppm/√Hz with respect to the total output EMF of 7 mV taking square characteristic of TC into account. In the case of PTB-type MJTC which has input impedance of 700 ohm, the contribution of the thermal noise is 0.02 ppm/√Hz with respect to the output EMF of 100 mV.

(3) Resolution of Detector

If we use a Keithley K182 nano-voltmeter as a detector, it has typical resolution of 14 nV/√Hz. This resolution amounts to 2 ppm/√Hz in the voltage resolution with respect to the total output EMF of 7 mV, or 1 ppm/√Hz in the resolution for the FRDC-DC difference measurement considering

the square characteristic of the EMF output. As in the case of ac-dc difference comparator described in chapter 3, the resolution of the detector dominates the over-all resolution of the measurement system. Though the resolution is ten times worse than that from the Johnson noise of the thermocouple, we can still obtain a standard deviation of 0.1 ppm for the FRDC-DC difference measurement using 100 s integration period. In the case of measurements with SJTCs, same type of nano-voltmeter designed for low-impedance measurement should improve the total resolution of the measurement system.

Typical example of reproducibility for the measured FRDC-DC difference for a SJTC is shown by **figure 8.18**. The measurements were repeated 45 times for the period of 64 hours. A reproducibility of 0.03 ppm (1σ) is obtained for each measurement. The type-A uncertainty for the average value is evaluated to be 0.03/√45=0.004 ppm (1σ)

8. 4. 2 Type-B uncertainties

(1) Effect of Imperfect Switching

The loss in the rms power due to the imperfectness of the switching is caused by the following two sources:

- (a) Threw rate of analog switches.
- (b) Switching-transients of the output circuit.

In the case of original waveform, the threw rate had a most significant effect because the waveform required the perfect switching. For example, if we choose switching frequency of 100 Hz, and if the edge rises or falls linearly with time during 10 ns, the loss of power is calculated as,

$$\Delta E \cong (2/3) \times (10 \text{ ns} / 10 \text{ ms}) \cong 0.7 \text{ ppm}$$

This effect increases linearly as the SW frequency is increased. In the case of modified waveform, the threw rate should not affect the measurement, since the same slope is reproduced for the CPDC modes and the MDFR modes.

The switching transient was also a big problem in the case of original waveform. In the actual situation, the effect of the transients can be much larger than the effect from the threw rate, and sometime it was possible to adjust the tran-

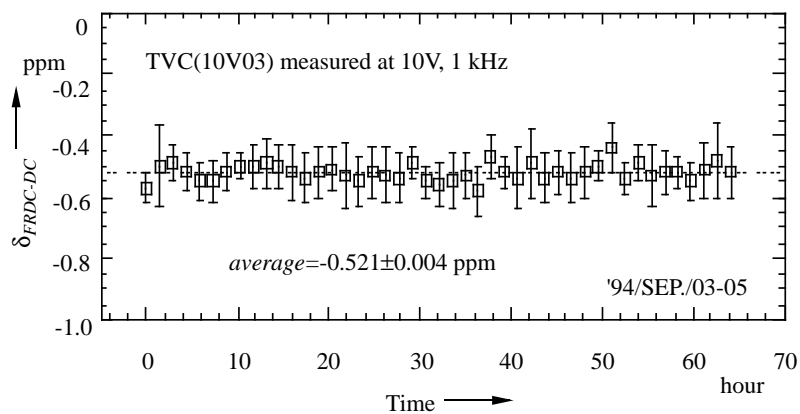


**Figure 8.18** Typical example of reproducibility for the measured FRDC-DC difference for a SJTC. A reproducibility of 0.03 ppm (1σ) is obtained.

sients to compensate the effects each other. In the case of modified waveform, the transients should not have any effect from its principle, so long as the same transients are reproduced for the CPDC modes and the MDFR modes.

#### (2) Memory Effect of Analog Switches

At the early stage of development of the FRDC source, we have experienced a linear dependence of FRDC-DC difference to the switching frequency, even using the modified waveform. As discussed in the section 4.4.1, we have traced the cause of this effect to a ‘memory-effect’ of the analog switches. When an analog switch change from ON state to OFF state, some charges are trapped in the FET channel. When the switch becomes ON state again, this charge is released and injected to the output current, resulting in the positive FRDC-DC difference proportional to switching frequency.

In the case of the new FRDC sources, a modified switching scheme described in section 4.4.2 are employed in order to suppress this effect. The analog switch, which connects the sources A/B to a TC, changes its state (ON/OFF) during a period when no voltage is applied to the switches. As a result, the memory-effect has been reduced within the resolution (0.1 ppm) of the system.

#### (3) Mismatching of Dummy Load Resistance

Another important experience we have encountered at the early stage of development is the effect of mismatching between the ‘dummy’ resistance and the input resistance of a TC. The mismatching of the resistance has caused an error in the current mode, and the effect was as large as a few ppm.

The main cause of this error was found out to be improper circuit design of the transconducting amplifier at the output circuit, as described in detail in section 5.4.2. After the improvement of the circuit, the effect was reduced within the resolution (0.1 ppm) of the system. This effect can be checked experimentally by intentionally mismatching the resistance of dummy loads.

#### (4) Interference Between the Sources

To obtain the equal RMS power for CPDC and MDFR modes, it is essential that there is no interference between the sources A and B. In order to avoid the possible interference between the two current sources, the sources A and B are electrically isolated using the optical isolators. The power supplies for those sources are also isolated using independent cores and magnetic shields, and the circuits of the sources A and B are separately shielded to reduce both thermal and electromagnetic couplings.

It is also possible to check the interference between the sources A and B experimentally, as described in 5.4.4. The result of such measurement confirmed the assumption that the effect of interference between the sources A and B is smaller than 0.1 ppm.

#### (5) Dielectric loss/absorption in the TC-input circuit.

When there is a dielectric loss or dielectric absorption in the TC-input, it can cause FRDC-DC difference which increases linearly with switching frequency, as described in section 5.4.3. This effect occurs at the current mode, and may cause error as large as a few ppm at switching frequency of 10 kHz. In order to reduce this phenomenon, the FRDC source uses Teflon PC board for the final output circuit. As a result, the effects have been reduced to less than 0.5 ppm at switching frequency of 10 kHz for 1 k $\Omega$  TC-input resistance. Since the effect is proportional to the input resistance, the effect becomes less than 0.1 ppm for thermal converters which have input impedance smaller than 200 ohm.

#### (6) Effect of off-time

If the period of the off-state  $t_{off}$  is not long enough to wait for the switching transient to die out, there is a possibility of correlation between the waveform from the sources A and B. Usually, the off-time of 10  $\mu$ s is long enough compared with 50 ns of the switching time of the IH5143 high-speed analog switches. If the off-time is not negligibly small compared with the time constant of joule heating  $\tau_{joule}$ , the EMF-output of the TC will be modulated by thermal ripple and may cause an error due to non-linearity of the system. These effects have also been checked experimentally by changing the off-time between 5 $\mu$ s to 200  $\mu$ s. No change in the FRDC-DC difference was detected with 0.1 ppm resolution.

When  $t_{off}$  is not negligibly small compared with the switching period  $T_{sw}$ , the effective power decreases as  $(1-t_{off}/T_{sw})$  and may cause an error due to level-dependence of TC to be measured. If we choose an off-time of 10  $\mu$ s, the loss of power is 1% at 1 kHz and as large as 10% at 10 kHz.

#### (7) Output resistance of the source

Since the output impedance of the FRDC source is not zero, the value obtained in the voltage mode deviate to the value obtained by current mode. The degree of the deviation is estimated by the ratio of output impedance of the source (0.1  $\Omega$ ) to the input resistance of the TVC (100  $\Omega$  to 10 k $\Omega$ ), and should be smaller than  $0.1\Omega/100\Omega = 10^{-3}$ . Similarly, the value obtained in the voltage mode deviate to the value obtained by current mode, due to the finite output impedance of the source. The degree of the deviation is estimated by the ratio of the input resistance of the TCC (10  $\Omega$  to 1 k $\Omega$ ) to the output impedance of the source (1M  $\Omega$ ), and should be smaller than  $1k\Omega/1M\Omega = 10^{-3}$ . Since the absolute values of FRDC-DC difference for normal TCs are smaller than 10 ppm, the deviation is estimated to be smaller than 0.1 ppm.

#### (8) Mismatching of rms power

As in the case of ac-dc difference comparator, mismatching of rms power between the FRDC mode and the dc mode can cause an error due to nonlinear output characteristic of the TC to be measured[32]. It is recommended that all the four sources (A $\pm$ , B $\pm$ ) should be adjusted to better than 100 ppm before each measurement. In this case, the effect to the FRDC-DC difference becomes less than 0.01 ppm.

#### (9) Higher Frequency Components

The rectangular waveform of the FRDC mode contains a large number of higher-frequency harmonics, and the power of the higher-frequency components can be by-passed through a shunt capacitance. In the case of original waveform, the power-loss due to shunt capacitance becomes significant even at switching frequencies as low as 100 Hz, as discussed in the sub-section 4.2.2. In the case of modified waveform, the effects of higher-frequency harmonics are mutually compensated between the CPDC modes and the MDFR modes. As was described in detail in section 6.3, the effect to the FRDC-DC difference becomes smaller than 0.01 ppm.

#### (10) Magnetic cable in the TC-input circuit.

Some types of RF coaxial cables use Cu coated Fe wires as the inner conductors. If these cables are used to connect the TVC with the FRDC source, it can cause FRDC-DC difference which increases linearly with switching frequency due to skin-effect. This effect occurs at the voltage mode, and becomes significant for TVCs with low input resistance ( $<100\Omega$ ). Other magnetic materials such as iron-clips should also be avoided. If these precautions are taken, the contribution from the skin-effect should be much smaller than 0.1 ppm.

#### (11) Linear dependence to switching frequency.

In the case of TCs or TVCs with low input resistance ( $<100\Omega$ ), linear dependence of FRDC-DC difference with switching frequency becomes significant. Most of the linear dependence is supposed to be contributed from the dielectric loss and the skin-effects inside the TCs or TVCs. Also some part of the effect seems to be contributed from the limited slew-rate of the OP amps in the voltage-feedback loop. Since this effect becomes significant only at higher frequencies ( $>1$  kHz), it is possible to separate this effect from the thermoelectric effect using the linear dependence. By excluding the linear dependence, the contribution to the FRDC-DC difference can easily be compensated to less than 0.1 ppm at relevant frequencies ( $<1$  kHz).

### 8. 4. 3 Criteria of measurement

Since the thermoelectric transfer difference of a TC can be determined with an accuracy better than 1 ppm, the FRDC source may be used as a basic reference in the ac-dc transfer standard. In such cases, the following four criteria should be examined for each measurement in order to secure the reliability of measurements.

- [1] The drift in the output EMF of TC stays less than 1 ppm/min during the measurement.
- [2] The FRDC-DC difference approaches to zero when switching frequency is reduced below the characteristic frequency [ $f_{SW} < (1/\tau_{TE})$ ].
- [3] The FRDC-DC difference stays at a constant value when switching frequency is increased above the char-

acteristic frequency [ $f_{SW} > (1/\tau_{TE})$ ].

- [4] No long-term drift in the measured FRDC-DC difference is observed.

In the case of relative measurement using an ac-dc comparator, the effect of temperature drift of the TCs can be mutually compensated if the two TCs have similar temperature coefficient. In the case of FRDC-DC measurement, such compensation does not occur and directly affect the measurement. Thus better stabilization of the ambient temperature is required in the FRDC-DC measurement than the case of relative ac-dc difference measurements. For example, after turning on the current to a new standard TVC of ETL, at least 30 minutes are required until the drift of EMF reduces to the allowable level.

The criteria [2] and [3] are based on the formula (6.15) derived in section 6.2.2. Slowly reversed FRDC waveform is equivalent to changing the mode between the DC(+) and DC(-) modes. Hence the FRDC-DC difference should approach to zero when switching frequency is reduced below the characteristic frequency. On the other hand, if the switching frequency is above the characteristic frequency, there is no contribution from the thermoelectric effects in the FRDC mode. Then the FRDC-DC difference should be equal to the thermoelectric transfer difference. However, in the case of measurements for MJTCs, linear dependence of the FRDC-DC difference to switching frequency is observed.

The criterion [4] is a convenient and very effective method to check the reliability of the FRDC-DC difference measurements, on the condition that there is no long-term drift in the ac-dc difference of the reference TC.

## 8. 5 Summary

Results of the experiments using the production-model (KST003) FRDC sources were reported. The FRDC-DC difference measurements have been performed for various kinds of SJTCs and MJTCs and the physical significance of the measured results was discussed. The large unexpected dependence of the FRDC-DC difference on the measurement modes was investigated in detail, and was explained by thermoelectric voltages in the input circuit due to the Seebeck effect. The sources of type-A and type-B components of the uncertainty in the FRDC-DC difference have been evaluated for the measurement with the FRDC source.

The effects of slew rate and transients at the time of switching, which have been the major source of uncertainties in the case of original FRDC waveform, are automatically compensated in the case of modified FRDC waveform. As a result, uncertainty for the type-B evaluation was reduced to be smaller than 0.3 ppm. The uncertainty for type-A evaluation was experimentally evaluated to be 0.03 ppm ( $1\sigma$ ) in the case of measurements with SJTC. Hence it is possible to evaluate the thermoelectric transfer difference with total uncertainty smaller than 1 ppm with the production model FRDC source.